Research Article

Open Access

Lucinaldo S. Silva, Luciano C. B. Lima, Francisco J. L. Ferreira, Mateus S. Silva, Josy A. Osajima, Roosevelt D. S. Bezerra, Edson C. Silva Filho*

Sorption of the anionic reactive red RB dye in cellulose: Assessment of kinetic, thermodynamic, and equilibrium data

Abstract: The cellulose matrix was characterized by FTIR, ^{13}C NMR, XRD, TG, SEM and applied in the removal of the reactive red RB dye in an aqueous medium, with a capacity of adsorption at a pH of 2.0, and an adsorption equilibrium time which was reached at around 200 mins. The kinetic study for the system followed the Elovich model. The adsorption isotherms for the system at temperatures of 35°C, 45°C, and 55°C were adjusted to the Langmuir, Freundlich, Sips, and Redlich-Peterson non-linear models, with a capacity of adsorption for adsorbent of 5.97 mg g^{-1}, 5.64 mg g^{-1}, and 4.62 mg g^{-1}, respectively. The adsorption occurred by electrostatic interactions and it was favorable and spontaneous, with the influence of temperature.

Keywords: cellulose, characterization, adsorption, anionic dye.

1 Introduction

Dyes are substances used in large-scale manufacturing, including the textile industry, the goal of which is to color their products. The textile dyes can be classified according to their chemical structure or method by which they are fixed. The use of dyes to color fabrics is a practice that has been used for a long time and which is supported by large quantities of dyes on the market. The dying process involves washing in its final stage of operation. The process is conducted in current baths for the removal of excessive original dye, or hydrolyzed dye that has not been fixed to the fiber in the previous stages due to the low fixation rates. About 10–15% of these dyes are discarded into effluents, polluting the environment and affecting aquatic organisms [1].

Additionally, most dyes have a synthetic origin, and the reactive red RB (Fig. 1) stands out, which presents in its structure aromatic rings, sulfonic groups and azos that are unlikely to reach oxidative catabolism and which are not biodegradable. Thereby, numerous techniques for their removal have caught chemists' attention, and many of them are still in the experimental stages of precipitation, photodegradation, membrane filtration, electrodeposition, coagulation [2]. However, many of these methods require additional chemicals or generate toxicants. Due to the high cost and complexity shown by these methods, adsorption is an alternative for the treatment of effluents contaminated with dyes [3].

Adsorption procedures are more advantageous in removing synthetic dyes from industrial effluents, because they are transferred from the aqueous effluent to a solid phase. This technique offers flexibility. The advantage of this method, when compared with others, is that in many
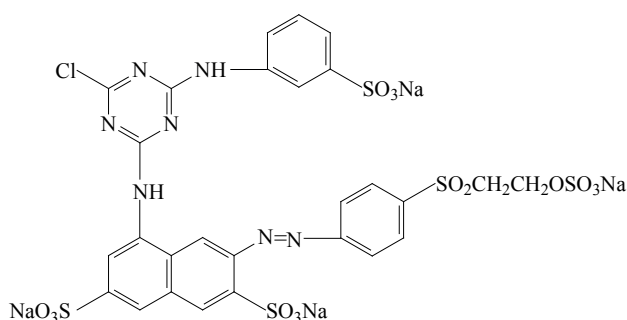
*Corresponding author: Edson C. Silva Filho:** IFPI, Federal Institute from Sciente and Thecnology from Piaui, 64600-000, Teresina, Piauí, Brazil, E-mail: edsonfilho@ufpi.edu.br
Lucinaldo S. Silva, Luciano C. B. Lima, Francisco J. L. Ferreira, Mateus S. Silva, Josy A. Osajima: LIMAV, Federal University of Piauí, 64049-550, Teresina, Piauí, Brazil
Roosevelt D. S. Bezerra: IFPI, Federal Institute from Sciente and Thecnology from Piaui, 64600-000, Teresina, Piauí, Brazil

Figure 1: Structure of the reactive red RB dye.

cases the treated effluent may be reused, is free of heat, odor, and specially, toxicity. Additionally, adsorption, most of the times, is a reversible process and adsorbent regeneration is possible creating a great operational saving. Nevertheless, some adsorption materials are limited due to economic reasons and have also a low reaction capacity [4].

The development of the chemistry of materials has triggered an increased interest for new, low-cost, renewable, low-toxicity materials, and has initiated studies of how to improve existing materials [4,5]. The most frequently studied materials are activated charcoal [6], cellulose [7], silica [8], clay [9], zeolites [10], chitosan [11], several lignocellulosic materials, agricultural waste, such as eucalyptus [12], wheat straw [12], sugarcane bagasse [13], peanut husk [14], bamboo [15], corn grains [16] among others. The cellulose stands out for being the most abundant polysaccharide in nature, and it arouses attention specially due to its low cost [1].

This work uses pure cellulose that was obtained commercially. It compares the results with data from the literature from various lignocellulosic materials used as adsorbents to identify whether the adsorption was influenced by the cellulose or other existing constituents in these materials.

This paper describes the adsorption of the reactive red RB dye in cellulose and the assessment of kinetic, thermodynamic, and equilibrium data.

2 Experimental part

2.1 Materials

Cellulose (Aldrich), HCl (Impex), NaOH (Impex), KNO_3 (Impex), reactive red RB dye (Dystar), and deionized water, all with analytical grade, were used with no previous purification.

2.2 Characterization

The infrared spectra were obtained using a Bomem FTIR spectrophotometer, MB series, by the tablet method, using 1% of the sample in KBr, with 32 scans, in the region between 4000 and 400 cm^{-1} with a resolution of 4 cm^{-1}. The solid form ^{13}C NMR spectra were obtained from cross-polarization (CP) with the magic angle of rotation spinning (MAS) technique in a Bruker AC 300 spectrometer, at room temperature, in a powder disc. The relaxation resting time

was 3 seconds, with an acquisition time of 50 ms, contact time of 3 ms, a rotation frequency of about 4 KHz, and a resonance frequency of 75 MHz. The X-ray diffraction was obtained on a Shimadzu instrument, model XD3 A, in the 2θ range between 5 and 50º, using the powder method. The scanning rate was 5º min^{-1}, using the CuKα radiation source, with a wavelength of 154.06 pm. The TG curve was obtained on a DuPont instrument, model 9900, at a temperature range between 25 to 1000°C, and at a heating rate of 10°C s^{-1}, using argon as carrier gas at a flow rate of 1.67 mL s^{-1}. The Scanning Electron Microscopy (SEM) was performed on a Jeol microscope, model JEOL JSM 6060, using the operational voltage of 20 kV with a 1000 to 5000 power of magnification.

2.3 Dye adsorption

2.3.1 pH measurements

The pH measurements were performed on a Tec-3MP pH meter, using a coupled glass electrode. The instrument calibration was carried out by using buffer solutions of pH 4.0 and 7.0.

2.3.2 Absorbance measurements

The absorbance measurements were performed on a Varian Cary 300 spectrophotometer, with a wavelength of 518 nm and a maximum solution absorption of the reactive red RB dye.

2.3.3 Point of zero charge (pH_{pzc})

The point of zero charge of the cellulose matrix (Cel) was determined by the method of solid addition [17]. 20.0 mL of a KNO_3 0.1 mol L^{-1} solution were added to a series of beakers. The pH value of each recipient was adjusted with HCl and/or NaOH 0.1 mol L^{-1} solutions for pH values from 2.0 to 12.0 and the solution's initial pH, pH_i, was measured. Next, 20.0 mL of each recipient containing KNO_3 were added to 20.0 mg of the cellulose matrix (Cel); the suspension was shaken for 24 h. After this time, the solution's final pH value, pH_f, was measured. The difference between the initial and the final pH was measured by $\Delta pH = pH_i - pH_f$. The graph of ΔpH in the function of pH_i was plotted; whereby the pH_i value of ΔpH was 0 and called the point of zero charge (pH_{pzc}) of the material.

2.3.4 Adsorption kinetics

Approximately 20.0 mg of the cellulose matrix was put in contact with 20.0 mL of a 30.0 mg L^{-1} solution of the reactive red RB dye, in the optimum pH of adsorption. This system was stirred every 20 minutes at the temperature of 25°C. After this period, the centrifugation was performed and an aliquot of the supernatant solution was removed, and the remainder quantity of dye was determined by the absorbance measurements. The result showed the necessary time to reach the maximum adsorption capacity of the adsorbent used [18]. The experimental data obtained was studied with the pseudo-first order [19], pseudo-second order [20], intra-particle diffusion [21], and Elovich [22] adsorption kinetic models.

2.3.5 pH influence

The variation study of the solution's initial pH of the reactive red RB dye was conducted t. For this study, dye solutions ranging from pH 2.0 to 12.0 were used so that the dye's initial concentration was 30.0 mg L^{-1}, as the analytical curve was within the range of 5-55 mg L^{-1}. With the pH adjusted within the above-mentioned range, the scanning was performed to check the dye's solutions spectra. 20.0 mL of the dye's solution was kept in contact with 20.0 mg of the matrix and stirred for 24 h, at a temperature of 25°C within the different pH values. After contact , centrifugation was carried out and an aliquot of the supernatant solution was removed, and the remainder quantity of dye was determined by absorbance readings. The result showed an optimum pH for adsorption [23,24]

2.3.6 Adsorption isotherm

A mass of approximately 20.0 mg of the cellulose matrix was placed in contact with 20.0 mL of a solution with different concentrations ranging from 200–900 mg L^{-1} of the reactive red RB dye. This system was continuously stirred at different temperatures (35°C, 45°C, and 55°C), in the pH and optimum adsorption time. After the optimum time, centrifugation was carried out and an aliquot of the supernatant solution was removed, and then the absorbance reading was performed. The non-linear models of Langmuir [25], Freundlich [26], Sips [27], and Redlich-Peterson [28] were applied to adjust the experimental data. The quantity of dye retained in the adsorbent q_e (mg g^{-1}) was calculated using Eq. 1:

$$q_e = \frac{(C_i - C_f)V}{m} \tag{1}$$

where C_i is the initial concentration of the dye (mg L^{-1}), C_f is its final concentration (mg L^{-1}), m is the mass of the adsorbent (mg), and V is the dye volume solution (mL) [29,30].

2.3.7 Statistical assessment of kinetic and equilibrium parameters

The assessment of the non-linear kinetic models and adsorption isotherms by the error function (F_{error}) represented by Eq. 2 were conducted, which compared the experimental data point by point with those obtained by the adjusted model. The models that had a lower value of F_{error} were the most adequate to describe the experimental behavior:

$$F_{error} = \sqrt{\sum_{i}^{p}\left(\frac{q_{i,\mathrm{mod}} - q_{i,\mathrm{exp}}}{q_{i,\mathrm{exp}}}\right)^2 \cdot \left(\frac{1}{p-1}\right)} \tag{2}$$

where $q_{i,mod}$ is the adsorbate adsorption capacity by the adsorbent provided by the model; $q_{i,exp}$ is the experimental adsorption capacity, and p is the number of experimental points performed [18,23].

The value of the correlation coefficient (R^2), provided by Origin 8.0, was also used to assess the adjustment, which could be determined by using equation 3.

$$R^2 = 1 - \left(\frac{\sum_{i}^{n}\left(q_{i,\mathrm{exp}} - q_{i,\mathrm{mod}}\right)^2}{\sum_{i}^{n}\left(q_{i,\mathrm{exp}} - \overline{q}_{i,\mathrm{exp}}\right)^2}\right) \cdot \left(\frac{n-1}{n-p}\right) \tag{3}$$

where $q_{i,exp}$ is the average of all values of $q_{i,exp}$ [18,23].

3 Results and discussion

3.1 Characterization

Fig. 2 shows the cellulose spectrum to qualitatively assess the presence of functional groups in the material. Thus, the spectrum indicates the presence of OH groups due to bands that appear in the region between 3600 and 3200 cm^{-1}, which are related to the OH stretching vibrations
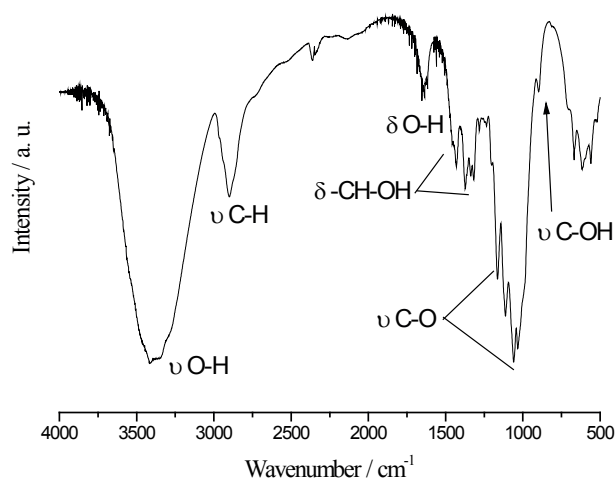
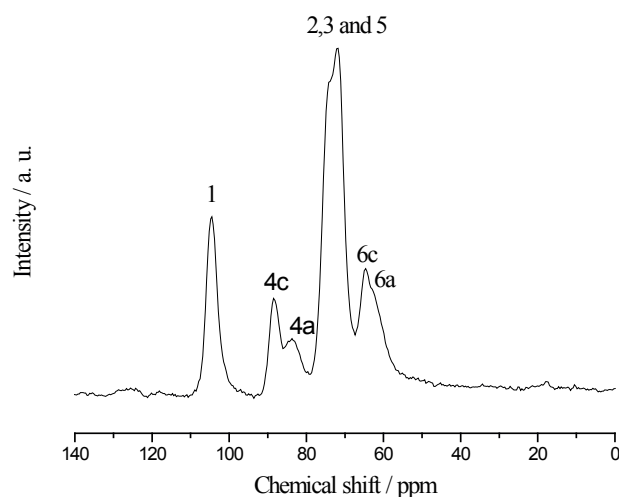**Figure 2:** Fourier Transform Infrared spectrum of celulose.
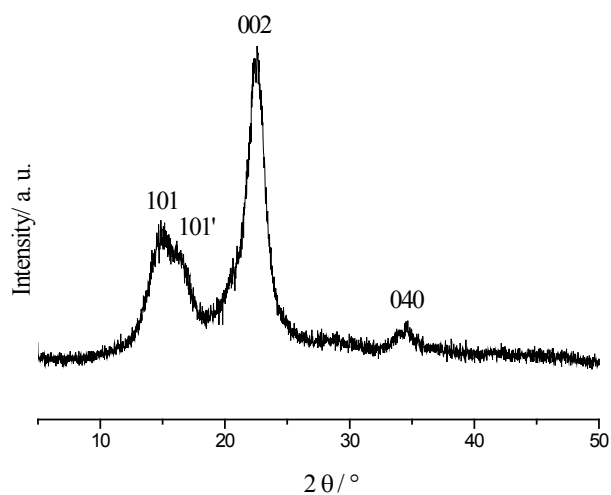

Figure 3: ^{13}C NMR spectrum of cellulose.

Figure 4: X-ray diffractogram of cellulose.

of the ring and the side chain υ(-CH-OH) and υ(-CH$_2$-OH). Another important vibration in the cellulose spectrum appears in approximately 2900 cm^{-1} corresponding to the stretching of the methyl and methylene groups. The absorption in the region between 3000–2800 cm^{-1} is assigned more precisely to υ C-H groups. The band in 1639 cm^{-1} corresponds to the vibration of deformation δ (O-H) of primary and secondary hydroxyl groups present in the cellulose structure. The region between 1500–1200 cm^{-1}, shows the presence of bands that also corresponds to the deformation of primary and secondary OH groups; between 1200–1000 cm^{-1} the stretching bands of (C-O) alcoholic groups occur. The bands present in the region below 1000 cm^{-1} are assigned to absorptions of the alcoholic groups [31,32].

The ^{13}C nuclear magnetic resonance spectrum, in solid state, enables the analysis of the chemical environment of the surface of cellulose chains. In the spectrum (Fig. 3), carbon 1 (C1) gives the highest chemical shift at 104 ppm, since it is bonded to two atoms of oxygen. The next two signals at 88 and 83 ppm are assigned to carbon 4 (C4) which appears to be bonded to only one oxygen atom. This is responsible for the 1,4'-β-glycosidic bond. The location of the signal at 88 ppm indicates a region of higher crystallinity and in 83 ppm, a region of lower crystallinity or amorphous. They are called 4c and 4a, respectively. The chemical shifts in the region 72–68 ppm are attributed to C2, C3, and C5 that have equivalent chemical environments (secondary carbons, bonded to –CH groups). The carbon that has the shortest chemical shift is C6, a primary carbon bonded to a hydroxyl group, which appears in 65 ppm (6c) for regions of higher crystallinity and in 63 ppm (6a), for regions of lower crystallinity [31,32].

Fig. 4 shows the X-ray diffractogram for the cellulose used in this work, showing three well-distinct planes 101, 002, and 040, characteristic of micro-crystalline cellulose. In crystalline regions, as the intermolecular interactions are more intense, and the arrangement more ordered, the availability of hydroxyls for chemical reaction is lower. In non-crystalline regions, these interactions are not as intense, the arrangement is not as ordered, and the hydroxyls are not as accessible to solvents or reagents any longer. The highest reactivity of the carbon 6 (C6) hydroxyl is due to the fact that it is primary and, therefore, less sterically hindered. The hydroxyls bonded to secondary carbons C2 and C3 are less reactive, probably because they are involved with intramolecular hydrogen bonds [5].

The thermogravimetric curve (TG) of cellulose is shown in Fig. 5. The curve shows a single decomposition event, in the temperature range between 290ºC and 374ºC, corresponding to a total mass loss of 92%, as we can see
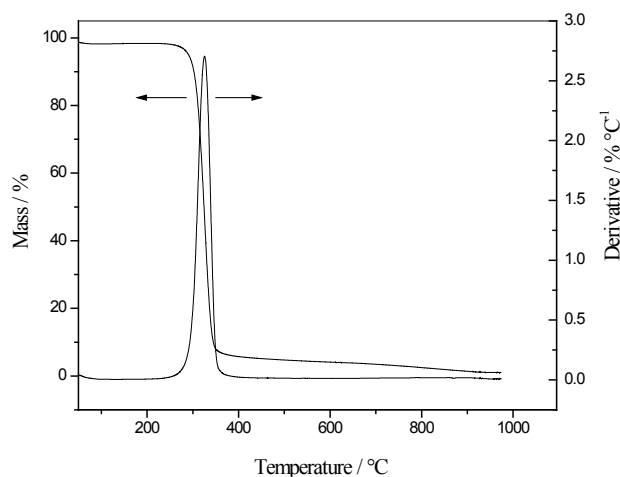
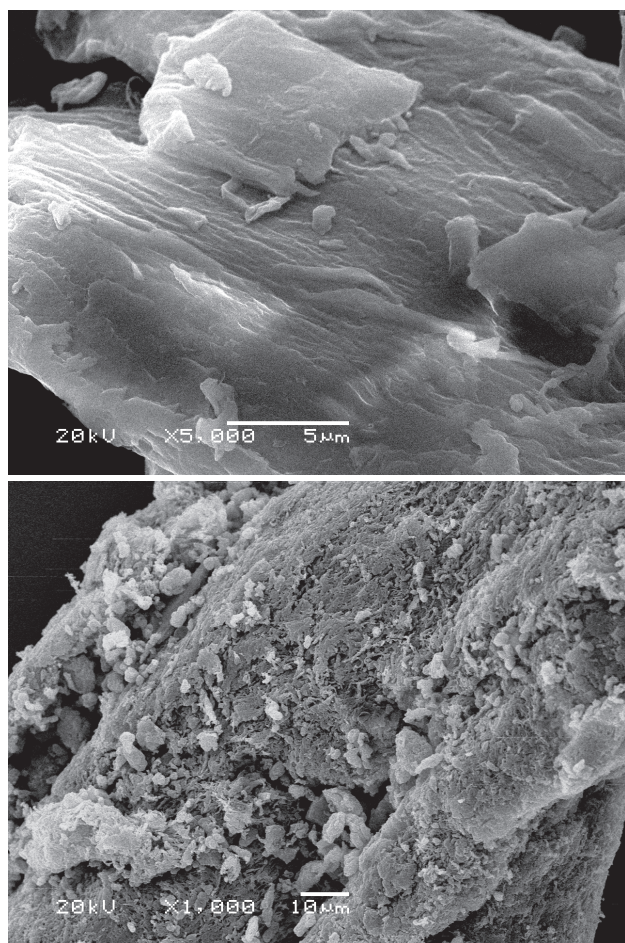**Figure 5:** Thermogravimetric curve and the derivative of cellulose.

Figure 6: Scanning Electron Microscopy (SEM) of cellulose.

from its derivative. However, it is clear that there is a 2% mass loss up to 70°C, corresponding to physisorbed water. The cellulose does not decompose totally in the above-mentioned temperature range, as up to 1000°C there is a 5% mass loss [4,5].

Fig. 6 shows the scanning electron microscopy of cellulose, which is a fibrous, compact, and almost amorphous material, with some cavities (micro-pores) that contributed to the adsorption of the reactive red RB dye in an aqueous solution.

The physical properties of this cellulose show that the area of cellulose is approximately $1\,m^2\,g^{-1}$, a low value when compared with inorganic materials, but consistent with several other biopolymers. This value can be confirmed when compared with the data for the distribution of pores (7000–50,000 nm) for these are in the region of macro-, micro- and mesoporous absence which greatly decreases the adsorption of nitrogen, thus providing a low surface area [33].

3.2 Dye adsorption

Fig. 7 shows the graph of a zero charge potential of the adsorbent matrix which shows the behavior of the cellulose surface's charge. As noted, in low pHs, small proton retention occurs by the material, with a slight increase in the pH_f value until the pH_i reaches 4. Thereafter, this retention gradually decreases until pH_i is around 6.5 in which the positive and negative charges are equivalent. This is the point we call point of zero charge, pH_{pcz}, which corresponds to the value where the curve intercepts the point where the pH variation is null. After this point, the material surface begins to release protons and consequently creates a reduction in the pH_f value. This process occurs until the pH_i reaches approximately 9.0, and after this point, the attraction of protons by the material surface starts again and, thus, the pH of the medium increases. After this behavior is verified on the matrix surface, the adsorption of cationic dyes is favored when the solution's pH is higher than the material's pH_{pcz}, whereas the adsorption of anionic dyes, such as the reactive red RB, is favored to a pH lower than the pH_{pcz} [34].

The behavior of the dye adsorption for the adsorbent matrix in function of time, was performed at room temperature. The quantity adsorbed became practically constant for the cellulose matrix with a pH of 2.0, after 200 minutes of contact with the adsorbent and the reactive red RB dye. This means that for the matrix, this time was adequate for the thermodynamic equilibrium to occur between the adsorbent and the adsorbate.

Aiming to establish the equilibrium for the maximum adsorption, different mathematical models were applied to explain the adsorption kinetics of the dye studied in the adsorbent matrix [19-22].
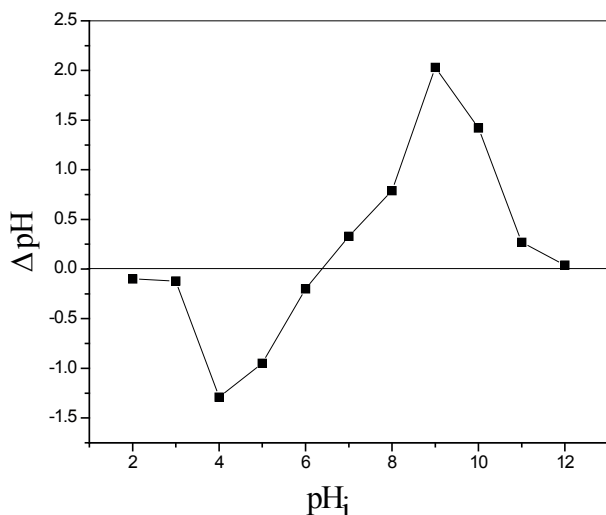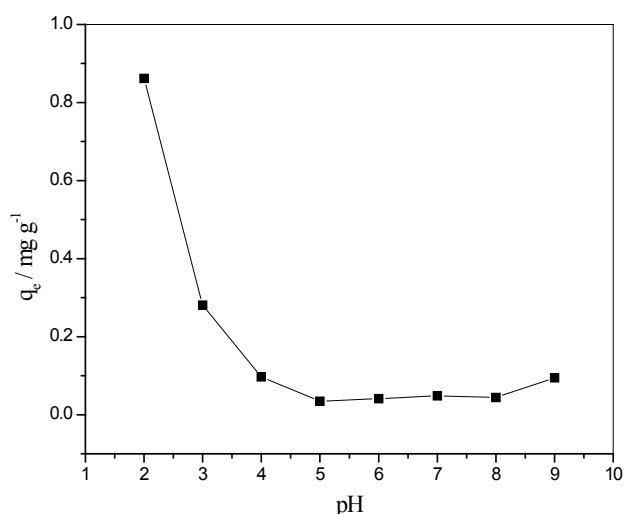
Figure 7: Potential of zero charge of cellulose.

Figure 8: Influence of pH on the adsorption of 30.0 mg L^{-1} of the reactive red RB dye in cellulose, T = 25°C.

The pseudo-first order model, also known as the Lagergren equation, is represented in a non-linear form by Eq. 4:

$$q_t = q_e \left[1 - \exp(-K_1.t) \right] \tag{4}$$

where q_e (mg g^{-1}) is the quantity adsorbed per gram of adsorbent in the equilibrium condition, q_t (mg g^{-1}) is the quantity adsorbed per gram of adsorbent in time t (min), and K_1 (min^{-1}) is the pseudo-first order adsorption velocity constant [19].

The pseudo-second order model, developed by Ho and McKay, is represented in a non-linear form by Eq. 5; the adsorption initial velocity, h (mg g^{-1} min^{-1}), where t = 0 can be obtained by Eq. 6:

$$q_t = \frac{K_2.q_e^{\,2}.t}{1 + q_e.K_2.t} \tag{5}$$

$$h = K_2 q_e^{\,2} \tag{6}$$

where q_e (mg g^{-1}) is the quantity adsorbed per gram of adsorbent in the equilibrium condition, q_t (mg g^{-1}) is the quantity adsorbed per gram of adsorbent in time t (min), and K_2 is the pseudo-second order velocity constant (g mg^{-1} min^{-1}) [20].

Another mathematical model applied was the intra-particle diffusion, represented by Eq. 7, aiming to identify a possible mechanism of intra-particle diffusion as a limiting stage:

$$q_t = K_p t^{1/2} + C \tag{7}$$

where Kp is the intra-particle diffusion constant (mg g^{-1} min$^{-1/2}$) and q_t is the quantity adsorbed (mg g^{-1}) in time t (min) [21].

The Elovich equation, represented by Eq. 8, is suitable for systems with heterogeneous adsorption surfaces involving a chemisorption process:

$$q_t = \frac{1}{\beta}(\ln \alpha \beta) + \frac{1}{\beta}(\ln t) \tag{8}$$

where β is the desorption constant (g mg^{-1}), α is the initial adsorption rate (mg g^{-1} min^{-1}), and q_t is the quantity adsorbed (mg g^{-1}) in time t (min) [22].

Table 1 shows the parameters obtained with the adjustment to the different kinetic models for the system studied in an aqueous medium. For this system, the correlation coefficient, showed R^2 < 0.95 for the matrix in the pseudo-first order models and intra-particle diffusion, and R^2 > 0.95 for the pseudo-second order models and Elovich as it can be seen in the adsorption of the reactive red 194 dye in Brazilian pine-fruit shells [18]. An adsorption process t follows them and shows the chemisorption as a limiting stage.

After the kinetics adsorption, the pH influence on the adsorption of the reactive red RB dye was performed on the cellulose surface with a pH variation from 2.0 to 12.0. However, it was observed that in the pH values of 10.0, 11.0, and 12.0 spectrum alterations regarding the changes in the maximum absorption wavelength occurred. Therefore, only the pH values between 2.0 and 9.0 were assessed. The experimental results related to the adsorption capacity in
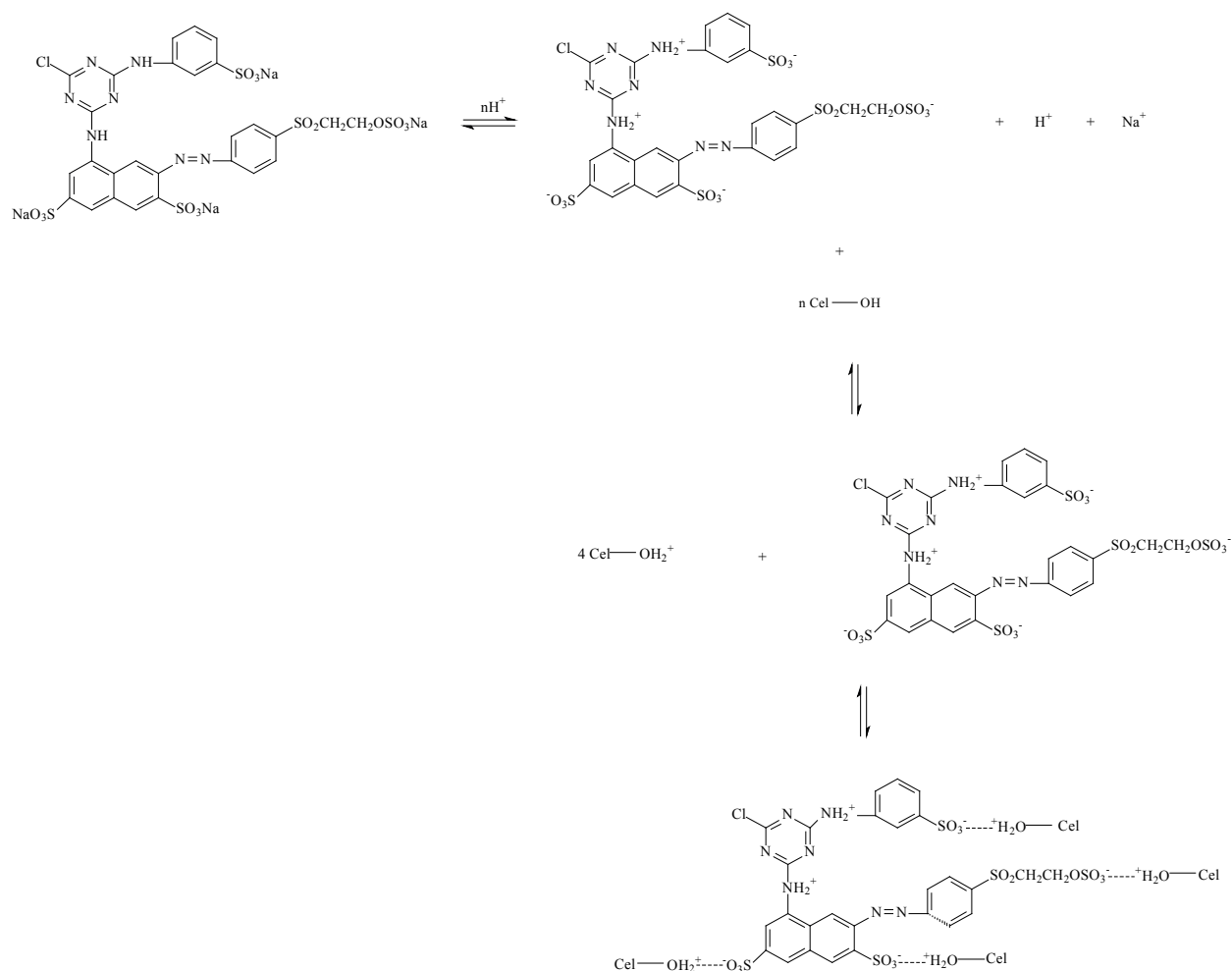
Figure 9: Diagram of the adsorption process of the cellulose matrix and the reactive red RB dye in an acidic medium.

the function of pH, show the influence of this property on the process involving the studied adsorbent, as illustrated by Fig. 8. The maximum adsorption capacity occurs at pH 2.0 for cellulose and will be considered for further studies [35].

As shown in Fig. 7, the quantity of adsorbed molecules in pH 2.0 is expected for the adsorbent matrix, as the pH_{pcz} is around 6.5. As long as the pH increases, the quantity of the adsorbed reactive red RB dye also increases. In Fig. 9, an interaction diagram illustrates that between cellulose and the anionic dye by electrostatic interactions, the dye was first deprotonated and then put in contact with the surface. The surface was protonated after the contact, and electrostatic interactions occurred which caused the removal of dye in an aqueous solution [35,36].

The pKa values for the anionic dyes that had sulfonic groups were lower than 2.0, whereas for those which had the azo groups were higher than 9.0. Thus, the reactive red RB dye that had such groups may

have appeared with positive and negative charges of pKa values between 2.0 and 9.0, and depending on the relationship between sulfonic and azo groups, the dye molecules may have presented neutral or negative charges, due to the higher quantity of sulfonic groups. Therefore, by correlating the values of pH_{PZC} (Fig. 7), pH (Fig. 8), and pKa a reaction diagram was proposed for the removal process of the reactive red RB dye in cellulose, as shown in Fig. 9 [37].

The experimental adsorption curves were performed in pH 2.0 for cellulose at temperatures of 35, 45 and 55°C, such as the adjustments to Langmuir [25], Freundlich [26], Sips [27], and Redlich-Peterson [28] non-linear models. Although the empirical models do not reflect the issues related to the adsorption mechanism, they provide information on the adsorbent's adsorption capacity [38,39].

The Langmuir isotherm is used for monolayer adsorption processes on homogeneous surfaces, in which the adsorption occurs in specific sites of the adsorbent.

Table 1: Kinetic parameters obtained with the different models for adsorption of 30.0 mg L^{-1} of the reactive red RB dye in the cellulose matrix, pH 2.0, T = 25°C.

Pseudo-first-order				
$q_{e(exp)}$ (mg g^{-1})	K_1 (min^{-1})	$q_{e(calc)}$ (mg g^{-1})	R^2	F_{error}
0.3343	0.0127	0.3528	0.9440	0.2853

Pseudo-second-order					
$q_{e(exp)}$ (mg g^{-1})	K_2 (g mg^{-1}min^{-1})	$q_{e(calc)}$ (mg g^{-1})	R^2	h (mg g^{-1} min^{-1})	F_{error}
0.3343	0.0288	0.4480	0.9545	0.0060	0.5235

Intraparticle diffusion		
K_P (mg g^{-1}min$^{-1/2}$)	R^2	F_{error}
0.2790	0.7126	10.8851

Elovich			
α (mg g^{-1}min^{-1})	β (g mg^{-1})	R^2	F_{error}
0.0130	10.2246	0.9583	0.1001

The expression of the Langmuir isotherm is represented by Eq. 9:

$$q_e = \frac{K_L q_{máx} C_e}{1 + K_L C_e} \tag{9}$$

where q_e is the quantity adsorbed of dye in the equilibrium (mg g^{-1}), C_e is the dye concentration in the equilibrium (mg L^{-1}), K_L is the Langmuir adsorption constant (L mg^{-1}), related to adsorption energy, and $q_{máx}$ is the maximum adsorption capacity (mg g^{-1}) [25].

The Langmuir parameters may be expressed in terms of a dimensionless separation factor, R_L, defined by Eq. 10, thus being possible assess the isotherm form:

$$R_L = \frac{1}{1 + K_L C_e} \tag{10}$$

where C_e is the dye concentration in the equilibrium (mg L^{-1}) and K_L is the Langmuir constant. For a favorable adsorption the values of R_L must be between 0 and 1 (0<R_L<1), whereas R_L > 1 represents an unfavorable adsorption; R_L = 1 represents a linear adsorption and for R_L = 0 the adsorption process is irreversible [25].

Another frequently applied model is the Freundlich isotherm, used to describe heterogeneous systems and represented by the empirical Eq. 11:

$$q_e = K_F C_e^{(1/n)} \tag{11}$$

where q_e is the quantity adsorbed of dye in the equilibrium (mg g^{-1}), C_e is the dye concentration in the equilibrium (mg L^{-1}), K_F (mg g^{-1}(mg L^{-1})$^{-1/n}$) is the Freundlich constant, related to the adsorption capacity, and n is the heterogeneity factor. Because they describe adsorption processes on heterogeneous surfaces, the adsorption sites have different adsorption energies that present a variation due to the surface covering. When the value of n for this model is equal to 1, the adsorption is considered linear, with identical adsorption energies in all sites; and for n greater than 1 the adsorption process is favorable [26].

The combination of the Langmuir and Freundlich models resulted in the Langmuir-Freundlich model, also known as Sips model, represented by Eq. 12:

$$q_e = \frac{K_E \, q_{máx} \, C_e^{\,n}}{1 + K_E \, C_e^{\,n}} \tag{12}$$

Table 2: Parameters obtained with different non-linear models of isotherms for adsorption of the reactive red RB dye in cellulose at different temperatures, pH 2.0.

Models	35°C	45°C	55°C
Langmuir			
$q_{máx}$ (mg g^{-1})	8.9438	8.4647	5.4743
K_L (L mg^{-1})	0.0029	0.0028	0.0011
R_L	0.3479	0.3978	0.6773
R^2	0.9907	0.9761	0.9865
F_{error}	0.0359	0.0566	0.6271
Freundlich			
n	2.4834	2.5451	5.2102
K_F (mg g^{-1}(mg L^{-1})$^{-1/n}$)	0.4257	0.4299	1.4030
R^2	0.9877	0.9677	0.9811
F_{error}	0.0389	0.0682	0.0535
Sips			
$q_{máx}$ (mg g^{-1})	6.9940	5.8655	4.6413
K_{LF} ((L g^{-1})$^{-1/n}$)	6.73x10^{-5}	1.70x10^{-9}	2.62x10^{-17}
n	1.7336	3.5928	7.3690
R^2	0.9899	0.9902	0.9999
F_{error}	0.0346	0.0329	0.0037
Redlich-Peterson			
K_{RP} (L g^{-1})	0.0149	0.0119	0.0218
a_{RP} (mg L^{-1})$^{-n}$	1.79x10^{-6}	4.39x10^{-11}	8.36x10^{-6}
n	1.9749	3.5147	1.9256
R^2	0.9922	0.9962	0.9967
F_{error}	0.0329	0.0200	0.0183

where q_e is the quantity adsorbed of dye in the equilibrium (mg g^{-1}), C_e is the dye concentration in the equilibrium (mg L^{-1}), K_{LF} is the Langmuir-Freundlich adsorption constant [(L g^{-1})$^{-1/n}$], $q_{máx}$ is the adsorption maximum capacity (mg g^{-1}), and n is the heterogeneity parameter. This model, at low concentrations, behaves similarly to the Freundlich model, considering the adsorption in multilayers. In high concentrations it follows the Langmuir model, considering the existence of a saturation point [27].

The Redlich-Peterson isotherm is another mathematical model used to characterize adsorption processes. It is represented by Eq. 13:

$$q_e = \frac{K_{RP} C_e}{1 + a_{RP} C_e{}^n} \tag{13}$$

where q_e is the quantity adsorbed of dye in the equilibrium (mg g^{-1}), C_e is the dye concentration in the equilibrium (mg L^{-1}), K_{RP} is the Redlich-Peterson adsorption constant

Table 3: Comparison of adsorption capacities of the anionic dyes by some adsorbents.

Adsorbent	Adsorbate	qe (mg g^{-1})	pH	Contact time	Reference
Wood sawdust (raw)	Acid blue 25	5.92	-	8 h	[40]
Banana pith	Acid brilliant blue	4.42	-	-	[42]
AC-Sugarcane bagasse	Acid orange 10	5.78	-	20 h	[43]
Coir pith (raw)	Acid violet	1.61	-	120 min	[44]
Blast furnace sludge	Acid yellow 36	1.40	7.0	180 min	[45]
Blast furnace sludge	Acid red 88	1.30	7.0	180 min	[45]
Blast furnace sludge	Acid blue 113	2.10	7.0	180 min	[45]
Fly ash	Metomega chrome Orange	0.74	-	110 min	[46]
Wollastonite	Metomega chrome Orange	0.70	-	150 min	[46]
Kaolin	Metomega chrome Orange	0.65	-	120 min	[46]
Coal	Metomega chrome Orange	0.77	-	80 min	[46]
Cellulose	Reactive red RB	5.97	2.0	200 min	This work

(L g^{-1}), a_{RP} is the affinity coefficient (mg L^{-1})$^{-n}$, and n is the heterogeneity parameter [28].

Table 2 shows the parameter values of the Langmuir [25], Freundlich [26], Sips [27], and Redlich-Peterson [28] models for the reactive red RB dye in view of the adsorbent cellulose in an aqueous medium, studied in pH 2.0. It can be observed that the Redlich-Peterson and Sips models show the lowest F_{error} values and the highest values of correlation coefficients (R^2), calculated from the non-linear adjustment to the experimental data, as observed in the adsorption of the Brazilian pine-fruit shell [18] and in the adsorption of silica [40] for dyes. Although the Langmuir non-linear model has not adjusted well, the adsorption process is favorable ($0 < R_L < 1$). The same is observed for the Freundlich non-linear model. Regarding the three above-mentioned temperatures, the values of

Table 4: Thermodynamic parameters of the adsorption of the reactive red RB dye in cellulose, pH 2.0.

Temperature (°C)	ΔG^o (J mol^{-1})	ΔH^o (J mol^{-1})	ΔS^o (J mol^{-1} K^{-1})
35	- 55.34		
45	- 61.66	139.3	0.7
55	- 67.98		

4 Conclusion

The pure cellulose showed a good performance in view of adsorptive assays, showing itself compromised in removing the reactive red RB dye from an aqueous medium, considering that the pH 2.0 is optimum for the adsorbent; the study of the kinetic mechanism indicates that the adsorption process is in compliance with the Elovich kinetic model; and the isotherms in pH 2.0 in temperatures of 35, 45, and 55°C follow the Redlich-Peterson and Sips non-linear model, with an influence of the temperature in the adsorption process. According to the adsorptive assays, cellulose may be applied in the environment for removing dyes in an aqueous medium, as it is a very abundant material, easily obtainable, and renewable.

n are greater than 1, a fact also verified for the models that had the best non-linear adjustments. Table 3 shows that for the systems at temperatures of 35, 45, and 55°C, the temperature influences the adsorption of the adsorbent , as the quantity adsorbed in pH 2.0 was 5.97, 5.64 and 4.62 mg g^{-1}, respectively. The material has a good adsorption capacity when compared with several adsorbents (Table 3) for the determined pH conditions and contact time. Thus, it is possible to verify that the cellulose influences the adsorption of the dye, may be changed by other components present in the lignocellulosic materials, or have similar capacity to other material removal, as shown in Table 3.

The adsorption thermodynamic parameters, including Gibbs' free energy (ΔG^o), enthalpy (ΔH^o), and entropy (ΔS^o), were calculated through Eqs. 14 and 15, being (ΔH^o) and (ΔS^o) obtained by Vant't Hoff equation (Eq. 14) plotting the linear graphic log K_e versus 1 / T [41]:

$$\log K_e = \frac{\Delta S^o}{2,303R} - \frac{\Delta H^o}{2,303RT} \tag{14}$$

$$\Delta G^o = \Delta H^o - T\Delta S^o \tag{15}$$

where R is the gas constant (8, 314 J mol^{-1} K^{-1}), T is the temperature (K), K_e is the equilibrium constant to temperature T, calculated through Eq. 16:

$$K_e = \frac{q_e}{C_e} \tag{16}$$

where q_e is the quantity adsorbed in the equilibrium (mg g^{-1}) and C_e is the concentration in the equilibrium (mg L^{-1}) [41]. The negative values of ΔG^o (Table 4) indicate that the adsorption process of cellulose is spontaneous and favorable. A positive enthalpy value (ΔH^o) shows that the adsorption process is endothermic by nature. A positive entropy value (ΔS^o) represents an increase in the randomness of the system during the adsorption process [1]

References

[1] Wang L., Li J., Adsorption of C.I. Reactive Red 228 dye from aqueous solution by modified cellulose from flax shive: Kinetics, equilibrium, and thermodynamics, Ind. Crop. Prod., 2013, 42, 153-158.

[2] Gupta V.K., Suhas., Application of low-cost adsorbents for dye removal – A review, J. Environ. Manage., 2009, 90, 2313-2342.

[3] Neta J. J. S., Moreira G. C., Silva C. J., Reis C., Reis E. L., Use of polyurethane foams for the removal of the Direct Red 80 and Reactive Blue 21 dyes in aqueous medium, Desalination., 2011, 281, 55-60.

[4] Melo J. C. P., Silva Filho E. C., Santana S. A. A., Airoldi C., Maleic anhydride incorporated onto cellulose and thermodynamics of cation-exchange process at the solid/liquid interface, Colloid Surface A., 2009, 346, 138-145.

[5] Melo J. C. P., Silva Filho E. C., Santana S. A. A. Airoldi, C., Exploring the favorable ion-exchange ability of phthalylated cellulose biopolymer using thermodynamic data, Carbohydr. Res., 2010, 345, 1914-1921.

[6] Zhong Z., Yang Q., Li X., Luo K., Liu Y., Zeng G., Preparation of peanut hull-based activated carbon by microwave-induced phosphoric acid activation and its application in Remazol Brilliant Blue R adsorption, Ind. Crop. Prod., 2013, 37, 178-185.

[7] Xie K., Zhao W., He X., Adsorption properties of nano-cellulose hybrid containing polyhedral oligomeric silsesquioxane and removal of reactive dyes from aqueous solution, Carbohydr. Polym., 2011, 83, 1516-1520.

[8] Donia A. M., Atia A. A., Al-amrani W. A., El-Nahas A. M., Effect of structural properties of acid dyes on their adsorption behaviour from aqueous solutions by amine modified silica, J. Hazard. Mater., 2009, 161, 1544-1550.

[9] İyim T. B., Güçlü G., Removal of basic dyes from aqueous solutions using natural clay, Desalination., 2009, 249, 1377-1379.

[10] Alver E., Metin A.U., Anionic dye removal from aqueous solutions using modified zeolite: Adsorption kinetics and isotherm studies, Chem. Eng. J. 2012, 200, 59-67.

[11] Cestari A. R., Vieira E. F.S., Tavares A. M.G. Bruns, R. E., The removal of the indigo carmine dye from aqueous solutions using cross-linked chitosan—Evaluation of adsorption thermodynamics using a full factorial design, J. Hazard. Mater., 2008, 153, 566-574.

[12] Robinson T., Mcmullan G., Marchant R., Nigam P., Remediation of dyes in textile e uent: a critical review on current treatment technologies with a proposed alternative, Bioresour. Technol., 2001, 77, 247-255.

[13] Zhang Z., O'Hara I. M., Kent G. A., Doherty W. O. S., Comparative study on adsorption of two cationic dyes by milled sugarcane bagasse, Ind. Crop. Prod. 2013, 42, 41-49.

[14] Gong R., Ding Y., Li M., Yang C., Liu H., Sun Y., Utilization of powdered peanut hull as biosorbent for removal of anionic dyes from aqueous solution, Dyes Pigments., 2005, 64, 187-192.

[15] Ip A.W.M., Barford J.P., Mckay G., Production and comparison of high surface area bamboo derived active carbons, Bioresour. Technol., 2008, 99, 8909-8916.

[16] Balathanigaimani M., Shim W., Park K., Lee J., Moon H., Effects of structural and surface energetic heterogeneity properties of novel corn grain-based activated carbons on dye adsorption, Micropor. Mesopor. Mat., 2009, 118, 232-238.

[17] Balistrieri L. S., Murray J. W., The surface chemistry of goethite (α − FeOOH) in major ion seawater, Am. J. Sci. 1981, 281, 788-806.

[18] Lima E.C., Royer B., Vaghetti J. C. P., Simon N. M., Cunha B. M., Pavan F. A., et al., Application of Brazilian pine-fruit shell as a biosorbent to removal of reactive red 194 textile dye from aqueous solution Kinetics and equilibrium study, J. Hazard. Mater., 2008, 155, 536-550.

[19] Largegren, S., About the theory of so-called adsorption of soluble substances, Kung. Suen Vetenskap. Dem. Handling., 1898, 241, 1–39.

[20] Ho Y. S., Mckay G., Kinetic models for the sorption of dye from aqueous solution by wood, Process. Saf. Environ., 1998, 76, 183-191.

[21] Weber Jr W. J., Morris J. C., Kinetics of adsorption on carbon from solution, J. Sanit. Engine Divis. Amer. Soc. Civil. Engin., 1963, 89, 31–59.

[22] Aharoni C., Tompkins F. C., Kinetics of adsorption and desorption and the Elovich equation, Adv. Catal. Rel. Subj., 1970, 21, 1–49.

[23] Machado F. M., Bergmann C. P., Fernandes T. H. M., Lima E. C., Royer B., Calvete T., et al., Adsorption of Reactive Red M-2BE dye from water solutions by multi-walled carbon nanotubes and activated carbon, J. Hazard. Mater. 2011, 192, 1122-1131.

[24] Shukla A., Zhang Y. H., Dubey P., Margrave J. L., Shukla S. S., The role of sawdust in the removal of unwanted materials from water, J. Hazard. Mater. 2002, 95, 137-152.

[25] Langmuir I., The constitution and fundamental properties of solids and liquids, J. Am. Chem. Soc., 1916, 38, 2221-2295.

[26] Freundlich H. M. F., Uber die adsorption in lösungen, Z. Phys. Chem. 1906, 57A, 385- 470.

[27] Sips, R., On the structure of a catalyst surface, J. Chem. Phys., 1948, 16, 490–495.

[28] Redlich O., Peterson D. L., A useful adsorption isotherm, J. Phys. Chem., 1959, 63, 1024-1024.

[29] Qin Q., Ma J., Liu K., Adsorption of anionic dyes onammonium-functionalized MCM-41, J. Hazard. Mater., 2009, 162, 133-139.

[30] Elkady M.F., Ibrahim A.M., Abd El-Latif M.M., Assessment of the adsorption kinetics, equilibrium and thermodynamic for the potential removal of reactive red dye using eggshell biocomposite beads, Desalination., 2011, 278, 412-423.

[31] Pavia D. L., Basser G. M., Morrill T. C., Introduction to Spectroscopy, 2rd ed., Saunders College Publishing, New York, 1996.

[32] Silva Filho E. C., Silva L. S., Lima L. C. B., Santos Junior L. S., Santos M. R. M. C., Matos J. M. E., et al., Thermodynamic data of 6-(4 -aminobutylamino)-6- deoxycellulose sorbent for cation removal from aqueous solutions, Sep. Sci. Technol. 2011, 46, 2566-2574.

[33] Bezerra R. D. S., Silva M. M. F., Santos M. R. M. C., Airoldi C; Silva Filho E. C., Natural cellulose for ranitidine drug removal from aqueous solutions, J. Environ. Chem. Eng., 2014, 2, 605-611.

[34] Srivastava V.C., Mall I.D., Mishra I.M., Characterization of mesoporous rice husk ash (RHA) and adsorption kinetics of metal ions from aqueous solution onto RHA, J. Hazard. Mater., 2005, 134, 257-267.

[35] Silva M. M. F., Oliveira M. M., Avelino M. C., Fonseca M. G., Almeida R. K., Silva Filho, E. C., Adsorption of an industrial anionic dye by modified-KSF-montmorillonite: Evaluation of the kinetic, thermodynamic and equilibrium data, Chem. Eng. J., 2012, 203, 259-268.

[36] Andrzejewska A., Krysztafkiewicz K. A., Jesionowski T., Treatment of textile dye wastewater using modified silica, Dyes Pigments., 2007, 75, 116-124.

[37] Almeida V.C., Development of analytical methods for the determination and extraction of textile dyes in industrial effluents, Doctoral Thesis, State University of Maringa, São Paulo, Brazil, 2006.

[38] Debrassi A., Largura M.C.T., Rodrigues C.A., Adsorção do Corante Vermelho Congo por Derivados da O-Carboximetilquitosana Hidrofobicamente Modificados, Quim. Nova., 2011, 34, 746-770.

[39] Maatar W., Alila S., Boufi S., Cellulose based organogel as an adsorbent for dissolved organic compounds, Ind. Crop. Prod., 2013, 49, 33-42.

[40] Gay D.S.F., Fernandes T.H.M., Amavisca C.V., Cardoso N.F., Benvenutti E. V., Costa T.M.H., et al., Silica grafted with a silsesquioxane containing the positively charged 1,4-diazoniabicyclo[2.2.2]octane group used as adsorbent for anionic dye removal, Desalination., 2010, 258, 128-135.

[41] Ruthven D. M., Principals of adsorption and adsorption processes, 1rd ed., Jonh Wley & Sons, New York, 1984.

[42] Namasivayam C., Prabha D., Kumutha M., Removal of direct red and acid brilliant blue by adsorption on to banana pith, Bioresour. Technol., 1998, 64, 77-79.

[43] Tsai W.T., Chang C.Y., Lin M.C., Chien S.F., Sun H.F., Hsieh M.F., Adsorption of acid dye onto activated carbons prepared from agricultural waste bagasse by ZnCl2 activation, Chemosphere., 2001, 45, 51-58.

[44] Namasivayam C., Dinesh Kumar M., Selvi K., Ashruffunissa Begum R., Vanathi T., Yamuna R.T., 'Waste' coir pith–a potential biomass for the treatment of dyeing wastewaters, Biomass Bioenerg., 2001, 21, 477-483.

[45] Jain A. K., Gupta V.K., Bhatnagar A., Suhas A., Utilization of industrial waste products as adsorbents for the removal of dyes, J. Hazard. Mater., 2003, 101, 31-42.

[46] Gupta G.S., Shukla S.P., An inexpensive adsorption technique for the treatment of carpet effluents by low cost materials, Adsorpt. Sci. Technol., 1996, 13, 15-26.